Proof of Lemma 2: We first focus on the case that users are scheduling according to $|h_K|^2 \geq \cdots \geq |h_1|^2$. Recall that for such an addressed multiple-access channel, the optimal detection strategy is to first detect s_k whose SNR, i.e., $\text{SNR}_k = (1/[(\mathbf{H}^H\mathbf{H})^{-1}]_{k,k})$, is the largest. Then, successive detection can be realized by removing the detected messages. We first show that SNR_1 is the maximum among SNR_k, $1 \leq k \leq K$. Then, prove that the diversity gain associated with SNR_1 is 1.

Consider a general $n \times n$ tridiagonal channel matrix $\mathbf{A}_n$ shown in (8) and $\mathbf{A}_n^H\mathbf{A}_n$ shown in (9). The inverse of $\mathbf{A}_n^H\mathbf{A}_n$ can be shown as

$$\left(\mathbf{A}_n^H\mathbf{A}_n\right)^{-1} = \begin{bmatrix} \mathbf{B}_{(n-1)\times(n-1)} & \mathbf{b}_{(n-1)\times 1} \\ \mathbf{b}^H_{(n-1)\times 1} & x_n^{-1}, \end{bmatrix} \tag{24}$$

where we recall that $x_n = (1/[\mathbf{A}_n^H\mathbf{A}_n]^{-1}_{n,n})$. Note that the submatrix $\mathbf{B}_{(n-1)\times(n-1)}$ can be calculated from the inverse of block matrices as

$$\begin{aligned}\mathbf{B}_{(n-1)\times(n-1)} &= \mathbf{A}_{n-1}^H\mathbf{A}_{n-1} + \mathbf{a}_n\mathbf{a}_n^H - \frac{1}{|a_n|^2}a_n\mathbf{a}_n a_n^*\mathbf{a}_n^H \\ &= \mathbf{A}_{n-1}^H\mathbf{A}_{n-1}.\end{aligned}$$

Therefore, we can have the following:

$$\text{SNR}_k = x_k$$

where $\mathbf{A}_k \triangleq \mathbf{H}_k$. On the other hand, from Proposition 1, we learn that

$$x_k = \frac{|h_k|^2 x_{k-1}}{|h_k|^2 + x_{k-1}} \tag{25}$$

which yields

$$\text{SNR}_k = \frac{|h_k|^2\text{SNR}_{k-1}}{|h_k|^2 + \text{SNR}_{k-1}} \leq \text{SNR}_{k-1}$$

which means that the SNR of s_1 is the largest and that s_1 needs to be detected first. Note that $\text{SNR}_1 = |h_1|^2$ results in a diversity gain of 1, that such a performance becomes the bottleneck of the system, and that the diversity gain of the worst user performance is therefore 1.

When the users are scheduled in a random way, consider that the user scheduled during the ith TS has the worst link to the destination. After the detection of s_k, $1 \leq k \leq (i-1)$, these $(i-1)$ messages are removed from the observation, and we have a $(K-i+1) \times (K-i+1)$ new channel tridiagonal matrix, whose element at its first row and first column is h_i, i.e., the worst channel. Following the given steps, we can again show that this user is the bottleneck of the system, which causes the worst achievable diversity gain to be 1. Therefore, the proof for the lemma is completed. ■

REFERENCES

[1] J. N. Laneman, D. N. C. Tse, and G. W. Wornell, "Cooperative diversity in wireless networks: Efficient protocols and outage behavior," *IEEE Trans. Inf. Theory*, vol. 50, no. 12, pp. 3062–3080, Dec. 2004.

[2] K. Azarian, H. E. Gamal, and P. Schniter, "On the achievable diversity-multiplexing tradeoff in half-duplex cooperative channels," *IEEE Trans. Inf. Theory*, vol. 51, no. 12, pp. 4152–4172, Dec. 2005.

[3] Z. Ding, K. K. Leung, D. L. Goeckel, and D. Towsley, "A novel relay assisted cooperative transmission protocol for wireless multiple access systems," *IEEE Trans. Commun.*, vol. 58, no. 8, pp. 2425–2435, Aug. 2010.

[4] Y. Liang and G. Kramer, "Rate regions for relay broadcast channels," *IEEE Trans. Inf. Theory*, vol. 53, no. 10, pp. 3517–3535, Oct. 2007.

[5] V. R. Cadambe and S. A. Jafar, "Interference alignment and the degrees of freedom for the K user interference channel," *IEEE Trans. Inf. Theory*, vol. 54, no. 8, pp. 3425–3441, Aug. 2008.

[6] E. Beres and R. Adve, "Selection cooperation in multi-source cooperative networks," *IEEE Trans. Wireless Commun.*, vol. 7, no. 1, pp. 118–127, Jan. 2008.

[7] X. Zhang, M. Hasna, and A. Ghrayeb, "Performance analysis of relay assignment schemes for cooperative networks with multiple source-destination pairs," *IEEE Trans. Wireless Commun.*, vol. 11, no. 1, pp. 166–177, Jan. 2012.

[8] T. Cover and J. Thomas, *Elements of Information Theory*, 6th ed. New York, USA: Wiley, 1991.

[9] Z. Ding, T. Wang, M. Peng, W. Wang, and K. K. Leung, "On the design of network coding for multiple two-way relaying channels," *IEEE Trans. Wireless Commun.*, vol. 10, no. 6, pp. 1820–1832, Jun. 2011.

[10] G. H. Golub and C. F. van Loan, *Matrix Computations*, 3rd ed. Baltimore, MD, USA: The Johns Hopkins Univ. Press, 1996.

[11] D. Tylavsky and G. Sohie, "Generalization of the matrix inversion lemma," *Proc. IEEE*, vol. 74, no. 7, pp. 1050–1052, Jul. 1986.

[12] H. A. David and H. N. Nagaraja, *Order Statistics*, 3rd ed. Hoboken, NJ, USA: Wiley, 2003.

A Frequency-Domain LOS Angle-of-Arrival Estimation Approach in Multipath Channels

Daniele Inserra, *Member, IEEE*, and
Andrea M. Tonello, *Senior Member, IEEE*

***Abstract*—In this paper, we deal with the line-of-sight angle of arrival (AoA) estimation in a multipath channel, assuming that the first arrival path (FAP) contains the AoA information. We consider pulse transmission with a low duty cycle from the source and reception using an antenna array. We propose a simple approach that comprises the following four steps: 1) coarse frame synchronization; 2) frequency-domain channel estimation; 3) frequency-domain identification of the FAP delay with a threshold-based method; and 4) AoA estimation from the FAP coefficient. We compare the method with the joint angle and delay estimation multiple-signal classification (JADE MUSIC) algorithm. Despite the high complexity of the JADE MUSIC, our approach exhibits smaller root-mean-square error (RMSE) in the AoA estimation for various multipath channel scenarios that are characterized by different values of delay spread and angular spread correlation.**

***Index Terms*—Angle-of-arrival (AoA) estimation, first-arrival-path (FAP) detection, frequency-domain channel estimation.**

I. INTRODUCTION

There are many application areas, e.g., vehicular and indoor people navigation, that can benefit from the use of radio localization systems to support not only navigation where the Global Positioning System does not guarantee coverage but also context-aware services that may require very short response times (e.g., safety applications [1]). Radio localization can essentially be performed using the following three techniques [2], [3]: 1) the signal strength (SS) technique, which estimates the distance of the transmitter node (the unknown position node) from the receiver node by exploiting a propagation-loss model; 2) the time-of-arrival (ToA) or time-difference-of-arrival technique,

Manuscript received August 8, 2012; revised December 10, 2012 and January 27, 2013; accepted January 27, 2013. Date of publication February 26, 2013; date of current version July 10, 2013. This work was supported in part by the Consorzio Nazionale Interuniversitario per le Telecomunicazioni (CNIT) under a Doctoral Research Grant. The review of this paper was coordinated by Dr. N.-D. Dao.

The authors are with the Dipartimento di Ingegneria Elettrica, Gestionale e Meccanica, Università degli Studi di Udine, 33100 Udine, Italy (e-mail: daniele.inserra@uniud.it; tonello@uniud.it).

Color versions of one or more of the figures in this paper are available online at http://ieeexplore.ieee.org.

Digital Object Identifier 10.1109/TVT.2013.2245428

which computes the wave propagation delay; and 3) the angle-of-arrival (AoA) method, which estimates the AoA of radio waves that impinge on an antenna array. To locate a node in a plane, three receiver nodes are required with the SS and ToA methods, whereas two receiver nodes are required with the AoA method, each having at least two colocated antennas. These methods need to work in a line-of-sight (LOS) propagation condition; otherwise, their performance can significantly degrade.

In this paper, we consider the AoA estimation in a multipath (MP) channel, a scenario that severely affects the algorithm precision [4]. In fact, even the well-known multiple-signal classification (MUSIC) [5] and estimation of signal parameters via rotational invariance technique (ESPRIT) [6] algorithms, which are used to determine the AoA of different sources, suffer the presence of MP propagation, because these methods fail to span the signal subspace in the case of correlated waves. To deal with this problem, some preprocessing technique such as spatial smoothing [7] can be applied to decorrelate the sources. Spatial smoothing may reduce the effective size of the array, and to properly work, the number of channel paths must be known. Alternatively, maximum-likelihood AoA estimation can be used [4], although it introduces high complexity. Another approach is the joint angle and delay estimation (JADE) method [8]. This technique jointly estimates AoAs and ToAs by computing the JADE MUSIC spectrum from the channel impulse response estimate. This method is subspace based, but it requires fewer antennas compared to other techniques. Moreover, with respect to (w.r.t.) the conventional MUSIC, it allows for associating the right AoA to each MP delayed component. However, the complexity is extremely high due to the need of computing the eigenvalue decomposition of a large matrix of size $MN \times MN$, where M is the number of antenna elements, and N is the duration of the channel in samples (which comprises the transmission waveform).

Motivated by the search of a simpler method, in this paper, we consider a frequency-domain approach for the AoA estimation in an MP channel that does not require any eigenvalue decomposition and does not need to know the number of channel echoes. It is assumed that the transmitter node sends a train of known pulses with a low duty cycle, i.e., each pulse is followed by a guard time to cope with the intersymbol interference introduced by the MP channel. We consider a sufficiently general channel model where each MP component has its own AoA and the FAP is the LOS component. Then, the receiver performs the following four tasks:

1) coarse frame synchronization;
2) frequency-domain channel estimation;
3) identification of the FAP with a threshold-based method;
4) AoA estimation from the FAP phase component.

Step 4 is accomplished by estimating the phase difference between the LOS signal components received by two adjacent antennas.

Note that our method is applicable regardless of the number of antennas (provided that it is at least equal to two) and the number of channel echoes, unlike the traditional subspace-based AoA estimation approaches [4]. Frequency-domain AoA estimation was also considered in [9]. This was done to resolve the frequency dependency of the phase when wideband transmission is considered in combination with a digital beamformer. Nonetheless, in this paper, we will consider signals with bandwidth such that this frequency dependency can be neglected.

This paper is organized as follows. Section II describes the system and the considered channel model. The AoA estimation algorithm is discussed in Section III. We show several numerical results in terms of the root-mean-square-error (RMSE) performance in Section IV. Finally, the conclusions follow.

II. System Model Description

Let us consider a scenario in which a single user transmits the radio frequency (RF) signal $x(t)e^{j2\pi f_c t}$, where f_c is the carrier frequency, to a base station that is equipped with a multiple-antenna array with M elements. The transmitted signal undergoes MP propagation so that the baseband channel impulse response for the ith antenna link can be written as

$$h^{(i)}(t) = \beta_0^{(i)}\delta\left(t-\tau_0^{(i)}\right) + \sum_{l=1}^{N_p-1}\beta_l^{(i)}\delta\left(t-\tau_l^{(i)}\right), i\in\{1,\ldots,M\} \quad (1)$$

where $\delta(t)$ is the Dirac delta, N_p is the number of paths, and $\beta_l^{(i)}$ is the complex amplitude of the lth path. The delay $\tau_l^{(i)}$ can be written as the sum of two contributions, i.e., $\tau_l^{(i)} = \tau_l + \Delta\tau_l^{(i)}$, where τ_l is the propagation delay from the user to the first element of the antenna array, whereas $\Delta\tau_l^{(i)}$ is the delay between the first and the ith elements due to a plane wave that impinges with angle ϕ_l. Note that, assuming a linearly equispaced antenna array, with the element spaced by $d = (\lambda_0/2)$, the delay $\Delta\tau_l^{(i)}$ is equal to $\Delta\tau_l^{(i)} = (i-1)\cos(\phi_l)/(2f_c), i \in \{1,\ldots,M\}$. Therefore, we obtain

$$\left|\Delta\tau_l^{(M)} - \Delta\tau_l^{(1)}\right| \le \frac{M-1}{2f_c} \quad \forall\, l \in \{0,\ldots,N_p-1\}. \quad (2)$$

Assuming that the signal bandwidth is BW and the sampling period T is chosen according to the Nyquist sampling theorem, i.e., $T = 1/(2\text{ BW})$, we can observe that the maximum delay difference $(M-1)/(2f_c)$ is negligible w.r.t. the sampling period T if and only if $(M-1)/(2f_cT) \ll 1$ and, thus, if and only if $(\text{BW}/f_c) \ll 1/(M-1)$. In the literature, this criterion is also referred to as the *narrowband* assumption [4]. Under this constraint, the channel model in (1) becomes

$$h^{(i)}(t) = \beta_0^{(i)}\delta(t-\tau_0) + \sum_{l=1}^{N_p-1}\beta_l^{(i)}\delta(t-\tau_l), i\in\{1,\ldots,M\}. \quad (3)$$

Note that we assume that the LOS component with delay τ_0 is always present. Then, under the narrowband assumption, the received signal at the ith antenna can be expressed as

$$y^{(i)}(t) = \beta_0^{(i)}x(t-\tau_0) + \sum_{l=1}^{N_p-1}\beta_l^{(i)}x(t-\tau_l) + w^{(i)}(t), \quad i\in\{1,\ldots,M\} \quad (4)$$

where $w^{(i)}(t)$ is the background noise that is assumed to be white Gaussian. The gains $\beta_l^{(i)}$ take into account the RF carrier phase rotation (as shown in the following section), which depends on the AoA of the plane waves that impinge on the antenna array.

A. Spatial Channel Model

We assume a sufficiently general channel model where the FAP is the LOS component. A number of main scattering clusters are present, and each cluster generates an MP component. The complex amplitude of the lth MP component at the ith antenna can be expressed as

$$\beta_l^{(i)} = \alpha_l e^{-j\kappa d(i-1)\cos(\phi_l)},\ i\in\{1,\ldots,M\} \quad (5)$$

where $\kappa = (2\pi/\lambda_0)$, with $\lambda_0 = c_0/f_c$, and c_0 is the speed of light. According to (5), the path that is associated with the lth cluster has AoA ϕ_l. Furthermore, to account for scattering in each cluster, we assume the presence of the factor α_l with a Rayleigh distributed amplitude and uniform phase. Because the antennas are closely spaced,

α_l is identical for all antennas, i.e., the channel is spatially correlated. Note that (5) also holds true for the LOS component, with $\alpha_0 = 1$. To complete the model, we need to specify the angular statistics. A well-accepted distribution for ϕ_l is the zero-mean Laplace, as discussed in [10]. Other possible distributions have been proposed in [11] and [12]. Furthermore, there exists a correlation between the angular spread and the path delay [13]. In [13], the joint probability density function of the AoA and the ToA is derived under an elliptical scattering model. A more general treatment is done in [14], where the relation between the delay spread and the angular spread is studied. Based on the findings in [14], we propose to relate the angular spread of the lth path with its delay τ_l as follows:

$$\sigma_l = \sigma_{\max} e^{-\frac{\psi}{\tau_l - \tau_0}} \tag{6}$$

where the critical delay spread ψ, i.e., the key parameter for determining the rate of angular spread increase, and the maximum observable angular spread $\sigma_{\max}$ allow us to parameterize the model. Essentially, the relation (6) reflects the intuition that closely delayed paths exhibit smaller relative AoA differences.

Finally, the fading coefficients $\alpha_l, l \in \{1, \ldots, N_p - 1\}$ are assumed uncorrelated, with exponential power decay profile $\Omega_l \propto e^{-(\tau_l - \tau_0)/\Gamma}$. The interarrival path delays $\tau_l - \tau_0$ are considered deterministic, i.e., $\tau_l - \tau_0 = lT_{\text{path}}$, $l \in \{1, \ldots, N_p - 1\}$, whereas we assume that the FAP delay is uniformly distributed in the interval $[0, T_f - T_p)$, where T_f is the transmission frame duration, and T_p is the transmission pulse duration as described in the following section.

B. Transmitted Waveform: Impulsive Modulation

To estimate the AoA, the source node transmits a known waveform pattern in the form of a sequence of weighted pulses, i.e., binary pulse-amplitude modulation, such that the baseband transmitted signal can be written as [15]

$$x(t) = \sum_{k=0}^{L_{tr}-1} b_k g(t - kT_f) \tag{7}$$

where $b_k \in \{\pm 1\}$, $k \in \{0, \ldots, L_{tr} - 1\}$ are the training bits, $g(t)$ is the pulse waveform with duration T_p, and T_f is the frame duration (or the bit period). In this paper, we assume that $g(t)$ is the second derivative of a Gaussian pulse that reads

$$g(t) = \left[1 - \pi \left(\frac{t - T_p/2}{T_0}\right)^2\right] e^{-\frac{\pi}{2}\left(\frac{t - T_p/2}{T_0}\right)^2} \tag{8}$$

where T_0 represents the inverse of the pulse spectral occupancy (defining the spectral occupancy as the frequency at which the pulse amplitude is 30 dB below its peak value), and $E_g = \int_0^{T_p} g(t)^2 dt$ is the pulse energy. We assume a low-duty-cycle transmission so that the guard time $T_g = T_f - T_p$ is larger than the maximum channel delay $\tau_{N_p - 1}$. This is to avoid interpulse interference.

At the receiver, the downconverted signal can be expressed as

$$y^{(i)}(t) = \sum_{k=0}^{L_{tr}-1} b_k g_{EQ}^{(i)}(t - kT_f) + w^{(i)}(t) \tag{9}$$

where $g_{EQ}^{(i)}(t) = g(t) * h^{(i)}(t)$ is the equivalent impulse response that comprises the effect of the pulse waveform $g(t)$ and the channel impulse response $h^{(i)}(t)$ ($*$ represents the convolution). After the analog-to-digital conversion at sampling rate $T = (T_f/N)$, the signal in (9) becomes

$$y^{(i)}(nT) = \sum_{k=0}^{L_{tr}-1} b_k g_{EQ}^{(i)}(nT - kT_f) + w^{(i)}(nT) \tag{10}$$

where $g_{EQ}^{(i)}(nT)$ is the discrete-time version of the equivalent impulse response $g_{EQ}^{(i)}(t)$. For the performance results, it is useful to define the average signal-to-noise ratio (SNR; identical for all antennas) as $\text{SNR} = E_g/(T_f \cdot N_0)$, where the noise power is N_0.

III. AoA Estimation

The objective of the system is the estimation of the complex channel coefficients $\beta_0^{(i)}$, $i \in \{1, \ldots, M\}$ of the LOS component by processing the received signal samples in (4). Based on the channel coefficient estimates, it is possible to determine the AoA ϕ_0. If we assume the knowledge of the delay of the FAP, the coefficients $\beta_0^{(i)}$ can be obtained from an estimate of the channel-frequency responses $H^{(i)}(f)$ as follows:

$$\beta_0^{(i)} = h^{(i)}(\tau_0) = \int_{-\infty}^{\infty} H^{(i)}(f) e^{-j2\pi f \tau_0}\, df \tag{11}$$

i.e., simply as the integral of the channel-frequency response. The estimation of the channel in the frequency domain is a simpler and more effective task than operating in the time domain when the channel MP components have delays that are a fraction of the transmission pulse duration. In fact, operating in the frequency domain eases the pulse deconvolution and enables the channel estimation by processing each frequency bin independent of the others [16]. Furthermore, the delay τ_0 can also be estimated in the frequency domain, because it translates in a linear-phase component in the channel-frequency response. The main steps of the proposed algorithm, therefore, are listed as follows:

- coarse frame synchronization to coarsely detect the frame timing;
- frequency-domain channel estimation by exploiting the training signal;
- fine synchronization to precisely identify the FAP delay;
- AoA estimation.

The larger the pulse bandwidth and the sampling frequency are, the higher the system resolution will be; however, we can also exploit the fact that closely spaced MP components have the AoA very correlated.

A. Coarse Synchronization

To detect the frame timing, i.e., the position of the first training bit/pulse, coarse synchronization is first performed. We use a data-aided version, similar to the approach in [17]. The method is divided in two steps. The first step identifies the time instant $\tau_{\max}$ where the channel exhibits the highest energy. This is obtained as

$$\tau_{\max} = T \cdot \arg\max_{n \in \mathbb{Z}} \{\Lambda(nT)\}$$

$$\Lambda(nT) = \sum_{i=1}^{M} \left| \sum_{k=0}^{L_{tr}-1} b_k y^{(i)}(nT - kT_f) \right|^2. \tag{12}$$

Note that the signals from all antennas are combined. Once we have locked into the highest energy channel tap, we are sure that $\tau_0 \leq \tau_{\max}$ [18]. Thus, the second step of the coarse synchronization looks for the smallest time instant $\tau_{\text{start}} \leq \tau_{\max}$ that maximizes the energy

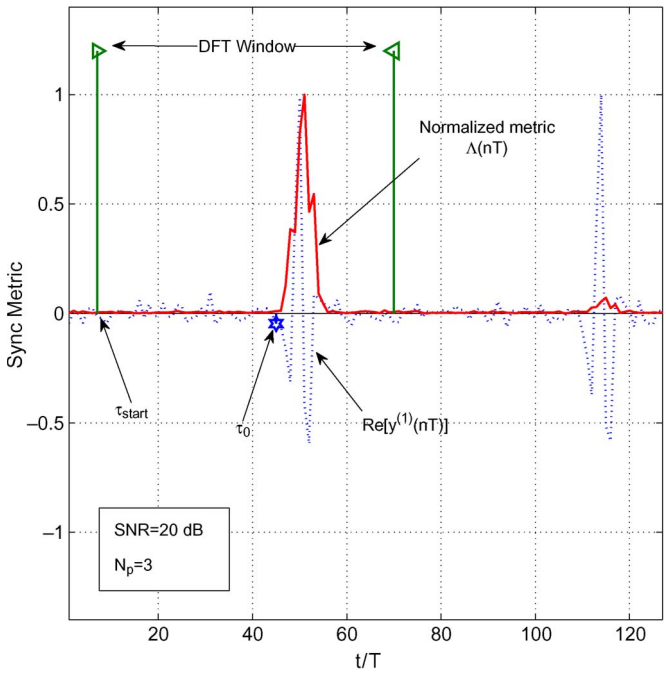

Fig. 1. Coarse-synchronization metric example.

collected within the window starting from τ_{start} and having duration $T_f = NT$, i.e.,

$$\tau_{\text{start}} = T \cdot \arg \max_{\frac{\tau_{\max}}{T} - N \le n \le \frac{\tau_{\max}}{T}} \left\{ \sum_{m=n}^{n+N-1} \Lambda(mT) \right\}. \quad (13)$$

One example of the coarse-synchronization metric is shown in Fig. 1, where we have assumed that SNR $= 20$ dB and $N_p = 3$.

B. Frequency-Domain Channel Estimation

Once we have located the window in which each frame is confined, i.e., $[\tau_{\text{start}}, \tau_{\text{start}} + T_f)$, the received and sampled signal in (10) delayed by τ_{start} becomes

$$\begin{aligned} \hat{y}^{(i)}(nT) &= y^{(i)}(nT + \tau_{\text{start}}) \\ &= \sum_{k=0}^{L_{tr}-1} b_k \hat{g}_{EQ}^{(i)}(nT - kT_f) + \hat{w}^{(i)}(nT) \end{aligned} \quad (14)$$

where $\hat{w}^{(i)}(nT) = w^{(i)}(nT + \tau_{\text{start}})$, and $\hat{g}_{EQ}^{(i)}(nT) = g_{EQ}^{(i)}(nT + \tau_{\text{start}})$.

Now, we need to estimate the channel-frequency response and to perform fine timing to identify the FAP component that has a delay equal to $\tau_0 - \tau_{\text{start}}$ w.r.t. the first sample in the window of samples (14). Without any loss of generality, we can assume that $\tau_{\text{start}} = 0$. We proceed by applying an N-point discrete Fourier transform (DFT) on the kth frame of the samples in (14) to obtain

$$Y_k^{(i)}(q) = b_k G_{EQ}^{(i)}(q) + N_k^{(i)}(q), \quad q \in \{0, \ldots, N-1\} \quad (15)$$

where $G_{EQ}^{(i)}(q) = G(q)H^{(i)}(q)$ is the DFT of the equivalent channel $\hat{g}_{EQ}^{(i)}(nT)$, $G(q)$ is the DFT of the pulse waveform $g(t)$, $H^{(i)}(q)$ is the DFT of the channel in (1) delayed by τ_{start}, and $N_k^{(i)}(q)$ is the DFT of the noise $\hat{w}^{(i)}(nT)$. To estimate the channel-frequency response $H^{(i)}(q)$, we consider the use of the recursive least square (RLS) algorithm [15], [17] on each frequency bin q from the DFT output in (15). As it is known, the RLS estimator has faster convergence than the somewhat simpler least mean square estimator. Note that this estimator independently operates over the N frequency bins. Let us denote with $\hat{H}_k^{(i)}(q)$ the channel estimate that was obtained at the kth iteration. Then, it can be computed as

$$\begin{aligned} \hat{H}_k^{(i)}(q) = \hat{H}_{k-1}^{(i)}(q) + e_k^{(i)}(q) K_k^{(i)}(q), \\ q \in \{0, \ldots, N-1\},\ i \in \{1, \ldots, M\} \end{aligned} \quad (16)$$

where the error $e_k^{(i)}(q)$ is defined as $e_k^{(i)}(q) = b_k Y_k^{(i)}(q) - \hat{H}_k^{(i)}(q)G(q)$. The kth Kalman gain for the ith antenna and the qth frequency bin is updated according to

$$\begin{aligned} K_k^{(i)}(q) &= P_{k-1}^{(i)}(q) G^*(q) \left(\lambda_{RLS} + P_{k-1}^{(i)}(q) |G(q)|^2 \right)^{-1} \\ P_k^{(i)}(q) &= \lambda_{RLS}^{-1} P_{k-1}^{(i)}(q) \left(1 - K_k^{(i)}(q) G(q) \right). \end{aligned} \quad (17)$$

The initial value $P_0^{(i)}(q)$ is set as $P_0^{(i)}(q) = 1/d_{RLS}$, where d_{RLS} has been assumed equal to 0.01 in all numerical examples. Furthermore, $\lambda_{RLS} = 0.999$.

In the following section, we simply refer to the result of the final iteration $\hat{H}_{Ltr}^{(i)}(q)$ as $\hat{H}^{(i)}(q)$.

C. Fine Synchronization

Now, the FAP delay can be estimated using the following metric:

$$\begin{aligned} \hat{\tau} &= \arg \min_{\tau \in [0, T_f - T_p]} \{\tau | \Lambda_h(\tau) > \gamma_{TH}\} \\ \Lambda_h(\tau) &= \frac{1}{M} \sum_{i=1}^{M} \left| \sum_{q=0}^{N-1} \hat{H}^{(i)}(q) e^{-j2\pi \frac{q\tau}{NT}} \right|^2 \end{aligned} \quad (18)$$

which corresponds to finding the phase for which the channel squared amplitude exceeds a threshold γ_{TH}. In addition, note that all antenna signals are combined. One illustrative example of the fine-synchronization metric is shown in Fig. 2. The choice of the threshold will be discussed in Section IV.

D. AoA Estimation

Having estimated the channel-frequency responses and the FAP delay, we can exploit the relation in (11) to estimate the LOS channel coefficients as follows:

$$\hat{h}_{\text{LOS}}^{(i)} = \sum_{q=0}^{N-1} \hat{H}^{(i)}(q) e^{-j2\pi \frac{q\hat{\tau}}{NT}}. \quad (19)$$

Based on $\hat{h}_{\text{LOS}}^{(i)}$, $i \in \{1, \ldots, M\}$, we simply estimate the AoA as

$$\hat{\phi}_0 = -\arccos\left(\frac{\angle z}{\kappa d} \right), \quad z = \frac{1}{M-1} \sum_{i=1}^{M-1} \hat{h}_{\text{LOS}}^{(i)} \cdot \hat{h}_{\text{LOS}}^{(i+1)^*}. \quad (20)$$

Note that the algorithm works independent of the number of MP components, e.g., also with a single LOS path.

IV. Numerical Results

In this section, we report several numerical results about the RMSE of the AoA estimation algorithm, which is defined as RMSE $= \sqrt{E\{|\phi_0 - \hat{\phi}_0|^2\}}$, where $E\{.\}$ is the expectation operator. To consider a reference method, we compare the proposed algorithm with the well-known JADE MUSIC method. Details about this method can be found in [8]. It comprises the following main steps:

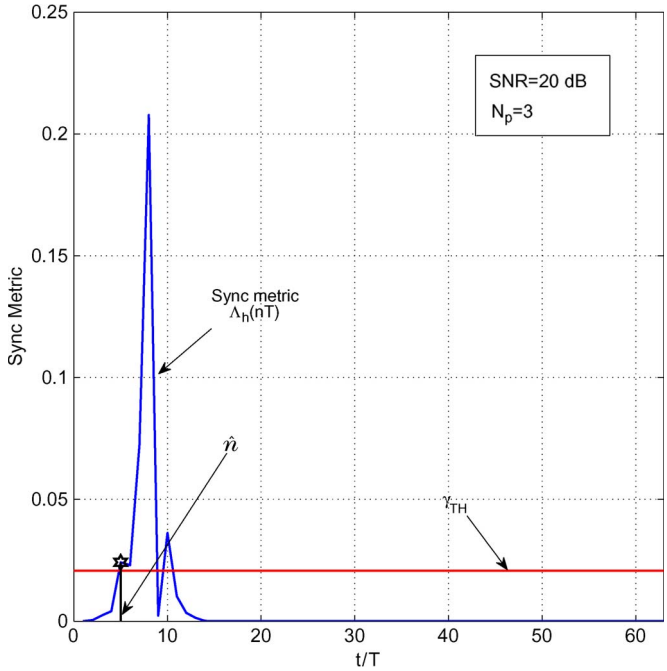

Fig. 2. Fine-synchronization metric example.

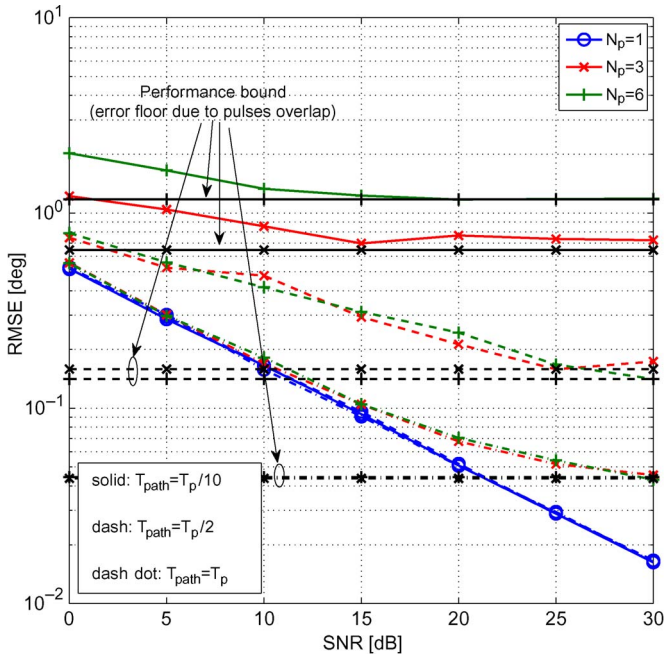

Fig. 3. RMSE as a function of SNR, with $N_p = \{1, 3, 6\}$, and different tap distances $(\{T_p/10, T_p/2, T_p\})$.

- a frame synchronization step that coarsely identifies the frame position;
- estimation of the channel impulse response (which comprises the transmitted pulse waveform);
- estimation of the autocorrelation matrix $R_{\hat{\mathbf{h}}\hat{\mathbf{h}}}$ of the extended channel impulse response $\hat{\mathbf{h}}$ obtained by stacking the channel impulse responses estimated from each antenna (with size MN);
- computation of the 2-D MUSIC spectrum, i.e., in both the spatial and temporal domains.

Note that JADE MUSIC identifies N_p peaks in its 2-D MUSIC spectrum. Hence, assuming that we have N_p channel paths, we look for the first one in the temporal dimension. We first perform coarse frame synchronization as in the proposed method. Then, we implement channel impulse response estimation through a least squares method, as shown in [8], weighting each frame with the corresponding training bit. Finally, an estimate of the autocorrelation matrix $R_{\hat{\mathbf{h}}\hat{\mathbf{h}}}$ is obtained.

A. AoA Estimation Performance Comparison

In the numerical examples, we have assumed a pulse with duration $T_p = 5T_0 = 100$ ns, which leads to a spectral occupancy of 50 MHz. The signal is upconverted at frequency $f_c = 2.412$ GHz. The array has size two, with spacing $d = (\lambda_0/2)$. The sampling period is $T = 10$ ns, and the frame has duration $T_f = 640$ ns, which gives $N = 64$ samples per frame. The training sequence length is $L_{tr} = 100$ bits. Note that these parameters ensure that the narrowband assumption holds true. Furthermore, in the channel model, we assume that $\Gamma = 4$, $\sigma_{\max} = 40^\circ$, and, where not specified, $\psi = 4$. Up to six channel paths are considered. The AoA is $\phi_0 = 30^\circ$ in all cases, except for the scenario analyzed in Fig. 6.

The threshold γ_{TH} is assumed as in [18], i.e., an intermediate level between the minimum and the maximum values of $\Lambda_h(nT)$. It can be written as

$$\gamma_{TH} = \min\{\Lambda_h(nT)\} + [\max\{\Lambda_h(nT)\} - \min\{\Lambda_h(nT)\}] \cdot \gamma_{TH,\text{norm}} \quad (21)$$

where $0 < \gamma_{TH,\text{norm}} < 1$ is the normalized threshold, which is the parameter used to set the final value. The effect of the threshold will be shown in Fig. 5. In all other figures, an optimal value obtained by simulation has been set.

Now, in Fig. 3, we report the RMSE of the proposed estimator as a function of the SNR. Different values of path interdistances T_{path} are assumed (they are defined as a fraction of the transmission pulse duration T_p). The figure shows that the MP channel introduces a loss in performance, which increases as the path interdistance decreases from $T_{\text{path}} = T_p$ to $T_{\text{path}} = 0.1T_p = T$. Nevertheless, the proposed estimator exhibits an RMSE that is below 1° for SNRs higher than 10 dB and $N_p \leq 3$, whereas the RMSE is slightly larger than 1° with $N_p = 6$. In this figure, we also report the performance curves obtained by assuming optimal synchronization and in the absence of noise. They represent the performance bounds that are achieved when there is some interference due to the pulses that overlap in MP propagation. As shown, the RMSE curves approach these bounds for high SNRs.

In the following discussion, we focus on the worst case MP channel whose paths are spaced by $T_{\text{path}} = 0.1T_p = T$, and we analyze the effect of the other parameters. In particular, in Fig. 4, the performance of the proposed AoA estimator as a function of both the SNR and the number of paths N_p is compared with the performance of the JADE MUSIC algorithm. In the ideal case $(N_p = 1)$, the two algorithms practically overlap. When the number of paths increases, we can observe that our method outperforms the JADE MUSIC, particularly for higher SNR values. In fact, even if JADE MUSIC can identify the temporal position of the FAP, it suffers the overlapping of pulses due to the presence of MP components with delays that are a fraction of the pulse duration. Our algorithm, instead, partially removes this effect and performs better. For high SNRs, both methods exhibit an error floor, which is approximately 1° for the proposed algorithm.

In Fig. 5, we analyze the RMSE as a function of the normalized threshold $\gamma_{TH,\text{norm}}$, with SNR $= \{20, 30\}$ dB, and different numbers of paths N_p. Note that the optimal threshold value depends on the channel parameters, whereas it does not significantly depend on the SNR. However, for all cases considered herein, the value $\gamma_{TH,\text{norm}} = 0.2$ is a good choice.

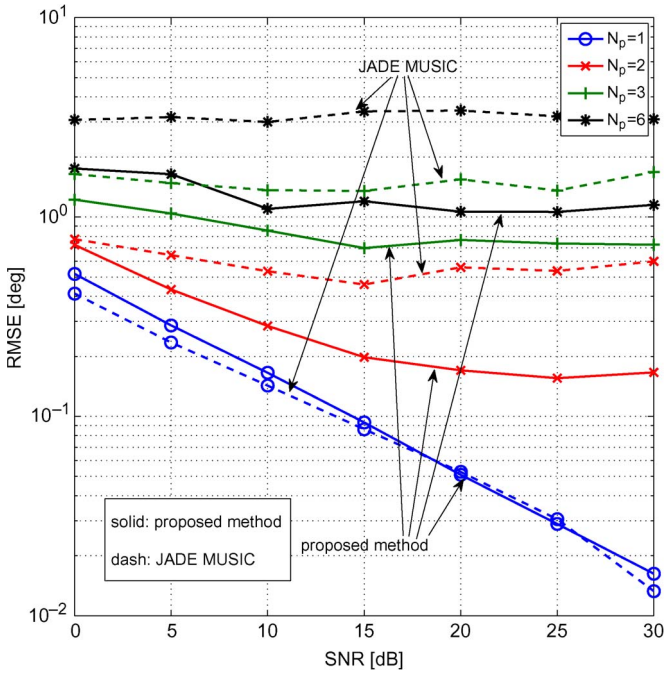

Fig. 4. RMSE as a function of SNR, with the proposed method and the JADE MUSIC.

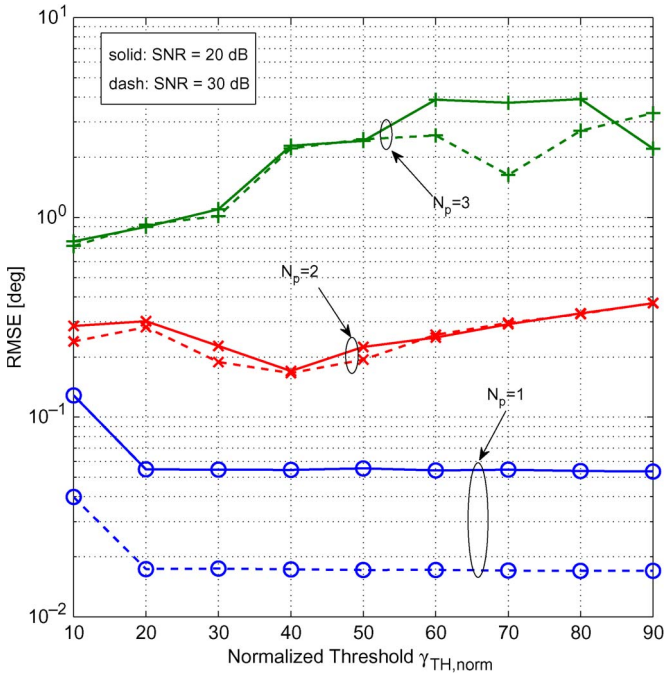

Fig. 5. RMSE as a function of the normalized threshold, with different SNRs and numbers of arrivals N_p.

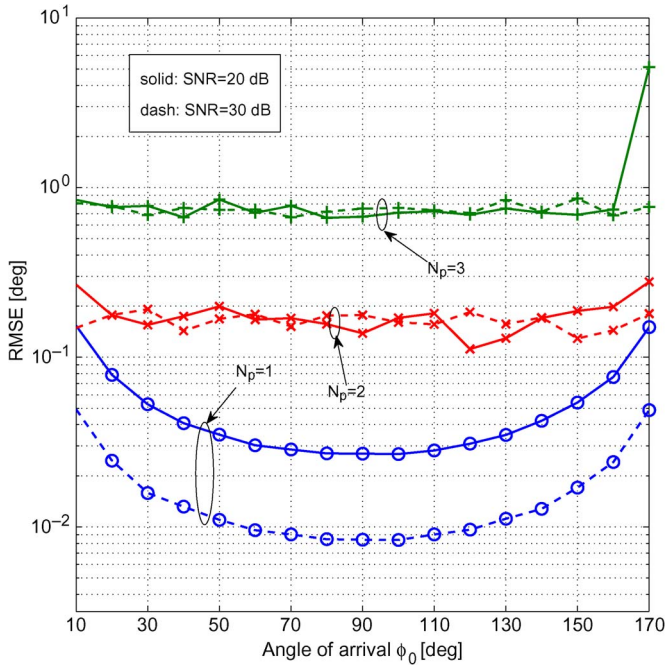

Fig. 6. RMSE as a function of the AoA ϕ_0, with different SNRs and numbers of arrivals N_p.

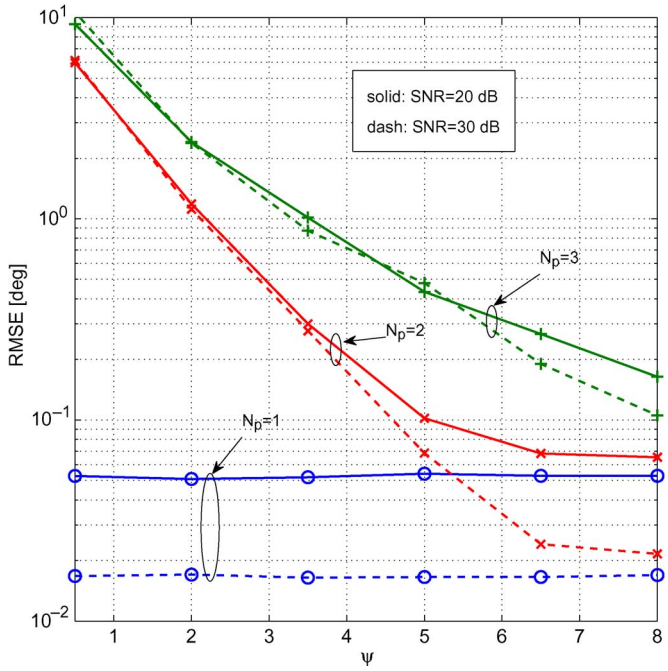

Fig. 7. RMSE as a function of ψ and the number of arrivals N_p, with different SNRs.

Fig. 6 shows the performance of our algorithm as a function of the AoA ϕ_0. With a single path, the performance is more influenced by the AoA. With multiple paths, the performance is less influenced by the AoA, because it is dominated by the ambiguity introduced by the multiple arriving paths, as also shown in Fig. 4.

In Fig. 7, the RMSE as a function of the critical delay spread ψ and the number of arrivals N_p is shown when an optimal threshold is chosen. Obviously, the curve $N_p = 1$ does not depend on the critical delay spread value. It can be observed that, with the increase of the number of arrivals N_p, the RMSE also increases. However, the increase of the critical delay spread is beneficial, because according to the model, this implies higher angular correlation between the MP components. Finally, it can be observed that the increase of the SNR can be beneficial, particularly in the cases $N_p > 1$, when the correlation of the MP component AoAs increases, i.e., when ψ increases.

B. Complexity Comparison

Note that JADE MUSIC needs the estimation of the autocorrelation matrix $R_{\hat{\mathbf{h}}\hat{\mathbf{h}}}$ that involves a computational complexity on the order of $\mathcal{O}(L_{tr}(MN)^3)$. Furthermore, the 2-D MUSIC spectrum needs to be computed on $(180/\Delta_\phi)N$ points, where Δ_ϕ is the desired angular resolution (in degrees), and it also requires eigendecomposition with

$\mathcal{O}((MN)^3)$ complexity. In the proposed method, instead, neither the autocorrelation matrix estimation nor the 2-D MUSIC spectrum computation is required. The overall complexities of the required fast Fourier transforms (FFTs), the RLS channel estimation, and the fine-synchronization step (inverse FFT plus search for the minimum) are, respectively, on the order of $\mathcal{O}(ML_{tr}N\log_2 N)$, $\mathcal{O}(ML_{tr}N)$, $\mathcal{O}(MN\log_2 N)$, and $\mathcal{O}(N)$. From this simple analysis, we can conclude that the proposed method provides lower computational complexity than JADE MUSIC.

V. Conclusion

We have considered a frequency-domain method for AoA estimation in an MP scenario by assuming a low-duty-cycle pulse transmission scheme. Estimation of the first arriving path phase and delay is done in the frequency domain. Several numerical results have been reported for different channel parameters, and they also show that the proposed method achieves good performance in MP channels. A comparison with the JADE MUSIC algorithm has revealed that, in the considered MP scenario characterized by path delays that are a fraction of the transmission pulse duration, better RMSE performance is reached despite its simplicity.

References

[1] Q. Xu, R. Sengupta, T. Mak, and J. Ko, "Vehicle-to-vehicle safety messaging in DSRC," in *Proc. 1st ACM Workshop VANET*, 2004, pp. 19–28.

[2] S. Gezici, Z. Tian, G. B. Giannakis, H. Kobayashi, A. F. Molisch, H. V. Poor, and Z. Sahinoglu, "Localization via ultrawideband radios," *IEEE Signal Process. Mag.*, vol. 22, no. 4, pp. 70–84, Jul. 2005.

[3] H. Tang, Y. Park, and T. Qiu, "A ToA-AoA-based NLOS error mitigation method for location estimation," *EURASIP J. Adv. Signal Process.*, vol. 8, no. 1, pp. 1–14, Jan. 2008.

[4] E. Tuncer and B. Friedlander, *Classical and Modern Direction-of-Arrival Estimation*. Burlington, MA: Academic, 2009.

[5] R. O. Schmidt, "Multiple emitter location and signal parameter estimation," *IEEE Trans. Antennas Propag.*, vol. AP-34, no. 3, pp. 276–280, Mar. 1986.

[6] R. Roy and T. Kailath, "ESPRIT—Estimation of signal parameters via rotational invariance," *IEEE Trans. Acoust., Speech, Signal Process.*, vol. 37, no. 7, pp. 984–995, Jul. 1989.

[7] T. J. Shan, M. Wax, and T. Kailath, "On spatial smoothing for direction-of-arrival estimation of coherent signals," *IEEE Trans. Acoust., Speech, Signal Process.*, vol. ASSP-33, no. 4, pp. 806–811, Aug. 1985.

[8] M. C. Vanderveen, C. B. Papadias, and A. Paulraj, "Joint angle and delay estimation (JADE) for multipath signals arriving at an antenna array," *IEEE Commun. Lett.*, vol. 1, no. 1, pp. 12–14, Jan. 1997.

[9] X. Huang, V. Dyadyuk, Y. J. Guo, L. Stokes, and J. Pathikulangara, "Frequency-domain digital calibration and beamforming with wideband antenna array," in *Proc. IEEE GLOBECOM*, Dec. 2010, pp. 1–5.

[10] R. J.-M. Cramer, R. A. Scholtz, and M. Z. Win, "Evaluation of an ultra-wideband propagation channel," *IEEE J. Sel. Areas Commun.*, vol. 50, no. 5, pp. 561–570, May 2002.

[11] R. Janaswamy, "Angle and time-of-arrival statistics for the Gaussian scatter density model," *IEEE Trans. Wireless Commun.*, vol. 1, no. 3, pp. 488–497, Jul. 2002.

[12] K. N. Le, "On angle-of-arrival and time-of-arrival statistics for geometric scattering channels," *IEEE Trans. Veh. Technol.*, vol. 58, no. 8, pp. 4257–4264, Oct. 2009.

[13] R. B. Ertel and J. H. Reed, "Angle and time-of-arrival statistics for circular and elliptical models," *IEEE J. Sel. Areas Commun.*, vol. 17, no. 11, pp. 1829–1840, Nov. 1999.

[14] G. D. Durgin, V. Kukshya, and T. S. Rappaport, "Wideband measurements of angle and delay dispersion for outdoor and indoor peer-to-peer radio channels at 1920 MHz," *IEEE Trans. Antennas Propag.*, vol. 51, no. 5, pp. 936–944, May 2003.

[15] J. G. Proakis, *Digital Communications*, 3rd ed. New York: McGraw Hill, 1995.

[16] M. V. Clark, "Adaptive frequency-domain equalization and diversity combining for broadband wireless communications," *IEEE J. Sel. Areas Commun.*, vol. 16, no. 8, pp. 1385–1395, Oct. 1998.

[17] A. M. Tonello and R. Rinaldo, "A time-frequency-domain approach to synchronization, channel estimation, and detection for DS-CDMA impulse-radio systems," *IEEE Trans. Wireless Commun.*, vol. 4, no. 6, pp. 3018–3030, Nov. 2005.

[18] I. Guvenc and Z. Sahinoglu, "Threshold-based TOA estimation for impulse radio UWB systems," in *Proc. IEEE ICUWB*, Zurich, Switzerland, Sep. 2005, pp. 420–425.

Low-Complexity Rate Selection of HARQ With Chase Combining in Rayleigh Block-Fading Channels

Seong Hwan Kim, *Student Member, IEEE*,
Seung Joon Lee, *Senior Member, IEEE*, and
Dan Keun Sung, *Senior Member, IEEE*

***Abstract*—We consider hybrid automatic repeat request with Chase combining (HARQ-CC) in a Rayleigh block-fading channel, where rate adaptation is based on long-term channel statistics instead of instantaneous channel information because the latter may be outdated. In the HARQ-CC with long-term rate adaptation, optimal selection of the transmission rate for each HARQ round requires a two-step numerical search procedure with heavy computational burden. In this paper, we propose two suboptimal rate-selection algorithms that substantially reduce the computational burden: In the first scheme, the solution of the second-step numerical search is approximated by using a closed-form Lambert W function, and in the second scheme, additionally, the solution of the first-step numerical search is approximated by a closed-form lower bound. Analytical and numerical results are presented to show that the proposed algorithms yield the performance of the long-term average transmission rate tightly approaching that of the optimal numerical search algorithm.**

***Index Terms*—Hybrid automatic repeat request (HARQ), rate selection, Rayleigh block fading.**

I. Introduction

Hybrid automatic repeat request (HARQ) schemes have attracted much attention because they significantly improve communication reliability, compared with simple ARQ schemes. In the HARQ scheme, a sender retransmits a part or the whole of a packet if acknowledgement is not fed back from a receiver. After retransmission, the receiver attempts to decode the packet by combining previously received signals with the new signal for the packet [1]–[3]. In particular, HARQ based on Chase combining (CC) has been widely used to retransmit the

Manuscript received March 6, 2012; revised September 3, 2012; accepted January 5, 2013. Date of publication February 7, 2013; date of current version July 10, 2013. This research was supported by the Ministry of Knowledge Economy, Korea, under the Information Technology Research Center support program supervised by the National IT Industry Promotion Agency (NIPA-2012-(H0301-12-1005)). The review of this paper was coordinated by Prof. Y. Su.

S. H. Kim and D. K. Sung are with the Department of Electrical Engineering, Korea Advanced Institute of Science and Technology, Daejeon 305-701, Korea (e-mail: shkim@cnr.kaist.ac.kr; dksung@ee.kaist.ac.kr).

S. J. Lee is with the Department of Electronics Engineering, Kangwon National University, Chuncheon 200-701, Korea (e-mail: s.j.lee@ieee.org).

Color versions of one or more of the figures in this paper are available online at http://ieeexplore.ieee.org.

Digital Object Identifier 10.1109/TVT.2013.2245691